

energy transition,  $40 \text{ cm}^{-1}$  for {CrCr}, is also inhomogeneous, similar to that for the unselectively excited luminescence spectrum.

When the absorption spectra in the region of  ${}^2E$  and  ${}^2T_1$  excitations (Figures 1 and 2) are compared, it is striking that  $\epsilon$  values are up to 5 times larger for {CrCr} than for {CrZn}. Since in both systems the transitions gain most of their intensities by a single-ion mechanism, we feel that the different behavior is due to the charge difference between the chromium(III) and zinc(II) neighbors of a given chromium(III). The higher charge of the neighbor gives rise to a larger electrostatic potential of ungerade parity at the site of the chromium(III) center, thus increasing the electric dipole transition moment of the otherwise parity-forbidden transitions. Different Cr-O and Cr-N distances in the molecular units may also contribute to the observed intensity differences.

Another interesting property to compare for {CrCr} and {CrZn} are the relaxation pathways for excited molecular units. There are essentially three possible mechanisms: (i) radiative relaxation, (ii) nonradiative multiphonon relaxation, and (iii) transfer of excitation energy to impurities and crystal imperfections acting as "killer" traps. These latter centers are excited by multistep nonradiative energy transfer from the genuine species and relax either nonradiatively or by emitting infrared photons.

(i) The radiative relaxation rate can be calculated from the observed oscillator strength of the lowest energy absorption origin and its vibrational sidebands.<sup>25</sup> The estimated values for the radiative lifetimes are on the order of 20 and 3 ms for {CrZn} and {CrCr}, respectively. They are 2 orders of magnitude longer than the measured lifetimes at 4.2 K: 230  $\mu\text{s}$  for {CrZn} and 72  $\mu\text{s}$  for {CrCr}. We conclude that radiative processes are not rate-determining and that quantum yields are of the order of 1% at 4.2 K.

(ii) Multiphonon relaxation rates are difficult to estimate, even for very simple high-symmetry complexes.<sup>26</sup> Here we only provide a qualitative argument, by which the observed faster decay of

{CrCr} by a factor of 3 can be rationalized. It has been experimentally shown<sup>27,28</sup> that the number of high-energy vibrators in the immediate environment of the excited center is an important determinant for multiphonon relaxation rates. O-H and C-H stretching vibrations are the dominating accepting modes in the title compounds. Their numbers are the same for the dimeric molecules in {CrCr} and {CrZn}. The essential difference is that in {CrZn} the electronic excitation is localized on the chromium(III) side of the molecule, whereas in {CrCr} it is delocalized over the whole molecule as a result of exchange interactions. In other words, the excited center has a larger spatial extension in {CrCr}, and as a consequence, a larger number of high-energy vibrators can contribute to the multiphonon relaxation process.

(iii) Nonradiative energy transfer to "killer" sites is assumed to occur with a rate determined by the rate of excitation energy migration within the genuine chromophores. It is obvious from Figure 7 that below 50 K the energy-transfer rate  $k_t$  in {CrZn} is higher than  $k$ , the reciprocal of the lifetime, by a factor of about 3.  $k$  is therefore not likely to be determined by trapping of the excitation at "killer" sites. The same conclusion is drawn for {CrCr} based on decay measurements over the inhomogeneously broadened luminescence origin region.

In conclusion, the comparative study of {CrCr} and {CrZn} has led to a deeper understanding of the manifestations of exchange interactions in {CrCr}. In addition energy-transfer processes resulting from intermolecular interactions as well as nonradiative relaxation processes have been elucidated.

**Acknowledgment.** We thank Hans Riesen for help with the luminescence line-narrowing experiments. The Swiss National Science foundation is acknowledged for financial support of this work. M.B. acknowledges support by the Dutch Foundation of Chemical Research (SON) with financial aid from the Dutch Organisation for Advancement of Pure Research (ZWO).

**Registry No.** {CrCr}, 110270-95-6; {CrZn}, 114378-26-6.

- (25) Imbusch, G. F. In *Luminescence Spectroscopy*; Lumb, M., Ed.; Academic: New York, 1978.  
 (26) *Radiationless Processes*; Di Bartolo, B., Ed.; Plenum: New York, 1980.

- (27) Kühn, K.; Wasgestian, F.; Kupka, H. *J. Phys. Chem.* **1981**, *85*, 665.  
 (28) Mvele, M.; Wasgestian, F. *Spectrochim. Acta, Part A* **1986**, *42A*, 775.

Contribution from the Department of Chemistry and Materials Science Center, Cornell University, Ithaca, New York 14853-1301

## $d^{10}$ - $d^{10}$ Interactions: Multinuclear Copper(I) Complexes

Kenneth M. Merz, Jr., and Roald Hoffmann\*

Received October 14, 1987

The unusual linear trinuclear Cu(I) complex  $[\text{Cu}(\text{tolyl}(\text{NNNNN})\text{tolyl})]_3$ , synthesized by Beck and Strähle, contains a remarkably short Cu-Cu separation of 2.35 Å. This makes it the natural subject of a molecular orbital investigation which is presented in this paper. The Cu-Cu interaction is attractive, as a result of  $s + p_z + d_{z^2}$  mixing, as for other  $d^{10}$  complexes. The stereochemical requirements of the ligand (we make a distinction between geometrical and electronic bite size) also favor the very short Cu-Cu separation. We also studied the hypothetical oligomers  $\text{Cu}_3(\text{RN}_2\text{R})_4^-$  and  $\text{Cu}_4(\text{RN}_2\text{R})_4$  as well as extrapolated polymers  $[\text{Cu}(\text{N}_2)_3]_n$  and  $[\text{Cu}(\text{N}_2)_4]_n$ . The latter should be conducting for most reasonable electron counts.

If the geometrical constraints of the ligand set allow it, Cu(I) complexes clearly express a tendency to cluster and polymerize.<sup>1</sup> The Cu-Cu distances observed in such oligomers and polymers range down to 0.2 Å shorter than the 2.56-Å separation in Cu metal. So the question is naturally raised as to the nature of the bonding interactions between Cu centers at such short distances.

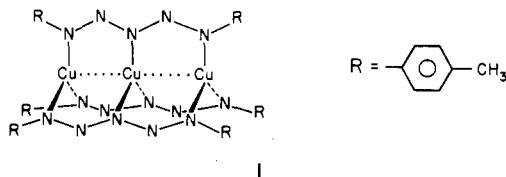
They cannot be repulsive. What could be done to make these Cu-Cu distances still shorter?

The answer to the first question has been given in our work and that of others:<sup>2</sup> there is mixing of 4s and 4p into 3d orbitals,

(1) For a recent survey on the chemistry of copper clusters, see: van Koten, G.; Noltes, J. G. *Comprehensive Organometallic Chemistry*; Wilkinson, G.; Stone, F. G. A., Abel, E. W., Eds.; Pergamon: Oxford, England, 1981; Chapter 14, pp 709-763.

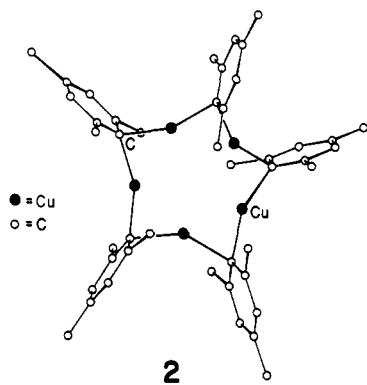
(2) (a) Mehrotra, P. K.; Hoffmann, R. *Inorg. Chem.* **1977**, *17*, 2187. (b) Dedieu, A.; Hoffmann, R. *J. Am. Chem. Soc.* **1978**, *100*, 2074. For other workers' theoretical contributions to bonding in  $d^{10}$ - $d^{10}$  systems, see: (c) Aydeef, A.; Fackler, J. P., Jr. *Inorg. Chem.* **1978**, *17*, 2182 and references cited therein. (d) Hollander, F. J.; Coucouvanis, D. *J. Am. Chem. Soc.* **1974**, *96*, 5646. (e) Mingos, D. M. P. *J. Chem. Soc., Dalton Trans.* **1976**, 1163.

converting repulsive d<sup>10</sup>-d<sup>10</sup> interactions into partial bonding. With respect to the second question, the design of optimal ligands, an important step was taken by Beck and Strähle recently, who reported a trinuclear Cu(I) complex with the pentaazenido ligand RNNNNNR<sup>-</sup> (**1**).<sup>3</sup>



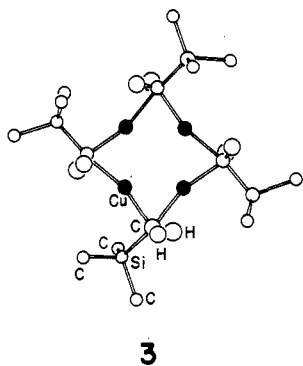
The world's record short Cu(I)-Cu(I) distance, 2.35 Å, is observed in this molecule. In this paper we examine the electronic structure of **1**. We also look at some hypothetical polymers related to this remarkable molecule. But before we do so let us review the structures of a few Cu(I) clusters that also have close Cu-Cu distances.

Gambarotta, Floriani, and co-workers<sup>4</sup> have recently reported the structure of an interesting pentameric species ([CuMes]<sub>5</sub>, **2**).



This structure is shaped like a five-pointed star with the mesityl groups serving as the outer points and the Cu(I) atoms as the inner points of the star. The average Cu(I)-Cu(I) distance is about 2.45 Å, which is 0.1 Å longer than that observed in **1**, but short enough to signal a fairly strong interaction between the Cu(I) atoms.

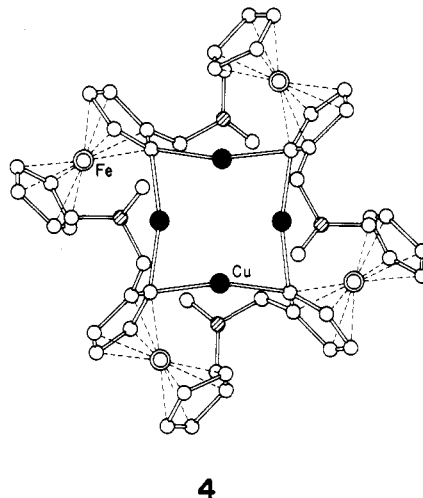
Earlier Jarvis, Lappert, and co-workers<sup>5</sup> found the structure of (Me<sub>3</sub>SiCH<sub>2</sub>Cu)<sub>4</sub> (**3**) to consist of a square planar array of Cu(I)



atoms bridged by alkyl groups. The interesting feature of this compound is the "puckering in" of the Cu(I) atoms, which results in a star-shaped (four points) structure. The distance between the Cu(I) atoms is 2.42 Å, which prior to the discovery of **1** was one of the shortest distances known. Extended Hückel MO calculations done by our group on **3** demonstrated that there is indeed a "soft" bonding interaction between the metal centers.<sup>2a</sup>

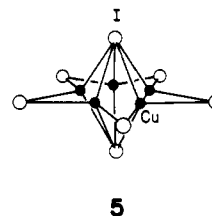
The bonding results from a mixing of the s, p, and d levels, which leads to an attraction between the Cu(I) atoms. Both the stereochemical requirements of the ligand and the direct Cu(I)-Cu(I) interaction contribute to the short metal-metal separation in **3**.

Another structure related to **3** is the one adopted by the mixed transition metal compound 2-cuprio-1-((dimethylamino)methyl)ferrocene (**4**).<sup>6</sup> This very beautiful structure is formed



by the action of 2-lithio-1-((dimethylamino)methyl)ferrocene on the complex of ((dimethylamino)methyl)ferrocene with copper iodide. Thus, **4** has as its bridging alkyl group a cyclopentadienide dianion moiety, which is then bound in an η<sup>5</sup> manner to Fe<sup>II</sup>Cp. The Cu-Cu distance is 2.44 Å.

Several very interesting structures have been observed for the iodocuprates(I) by Hartl and co-workers.<sup>7</sup> For example, [Cu<sub>5</sub>I<sub>7</sub>]<sup>2-</sup> has five CuI<sub>4</sub> tetrahedra condensed in a cyclic array, which leads to the idealized structure **5**.<sup>7a</sup> However, this idealized structure



would give extraordinarily short Cu(I)-Cu(I) distances (ca. 1.85 Å). The observed structure has the Cu atoms displaced above or below the I<sub>5</sub> plane, yielding a Cu-Cu distance of 2.58 Å, which is about the bond distance observed in copper metal.

Face-shared tetrahedra, an uncommon structural feature in coordination chemistry, are accommodated if the tetrahedra are centered by Cu(I) ions. Two examples, among several, are given by the Cu<sub>2</sub>I<sub>3</sub><sup>-</sup> chain **6**<sup>8a</sup> and the Cu<sub>3</sub>I<sub>4</sub><sup>-</sup> chain **7**.<sup>8b</sup> The shortest Cu-Cu separations are 2.45 Å in **6** and 2.46 Å in **7**.

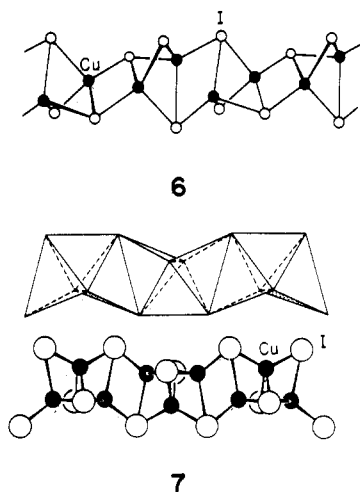
It is clear that in all of these structures there must be some Cu-Cu bonding interaction. The question remains: how much bonding? The 2.35 Å Cu-Cu distance in **1** is spectacularly short, by any measure. The ligand geometry is also highly symmetrical, and so this complex is a natural focus for a further examination of this bond type.

#### A Simple Picture of Attractive Cu(I) Interactions

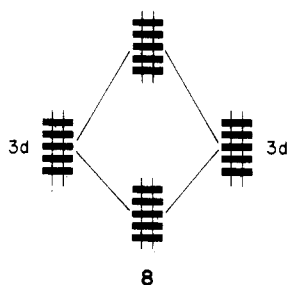
Before beginning an analysis of the Beck and Strähle complex **1**, it is useful to review the explanation that we have given for why Cu(I)-Cu(I) interactions are not repulsive.<sup>2</sup>

- (3) Beck, J.; Strähle, J. *Angew. Chem., Int. Ed. Engl.* **1985**, *24*, 409.  
 (4) Gambarotta, S.; Floriani, C.; Chiesi-Villa, A.; Guastini, C. *J. Chem. Soc., Chem. Commun.* **1983**, 1156.  
 (5) Jarvis, J. A. J.; Kilbourn, B. T.; Pearce, R.; Lappert, M. F. *J. Chem. Soc., Chem. Commun.* **1973**, 475.

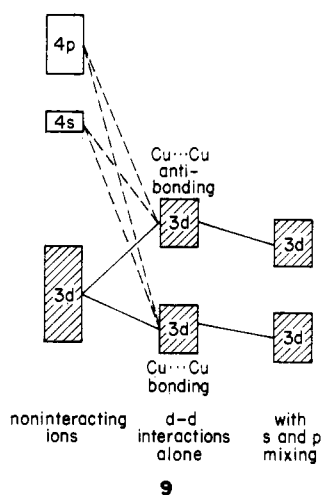
- (6) Nesmeyanov, A. N.; Struchkov, Yu. T.; Sedova, N. N.; Andrianov, V. G.; Volgin, Yu. V.; Sazonova, J. *Organomet. Chem.* **1977**, *137*, 217.  
 (7) (a) Hartl, H.; Mahdjour-Hassan-Abadi, F. *Angew. Chem., Int. Ed. Engl.* **1984**, *23*, 378. (b) Mahdjour-Hassan-Abadi, F.; Hartl, H.; Fuchs, J. *Angew. Chem., Int. Ed. Engl.* **1984**, *23*, 514.  
 (8) (a) Andersson, S.; Jagner, S. *Acta. Chem. Scand., Ser. A* **1985**, *A39*, 181. (b) Hartl, H.; Mahdjour-Hassan-Abadi, F. *Z. Naturforsch., B: Inorg. Chem., Org. Chem.* **1984**, *39B*, 149.



If two or more Cu(I) ions were represented well by only their closed  $d^{10}$  configurations, one would in fact get only a repulsion between them (8). In one-electron theory this is the consequence



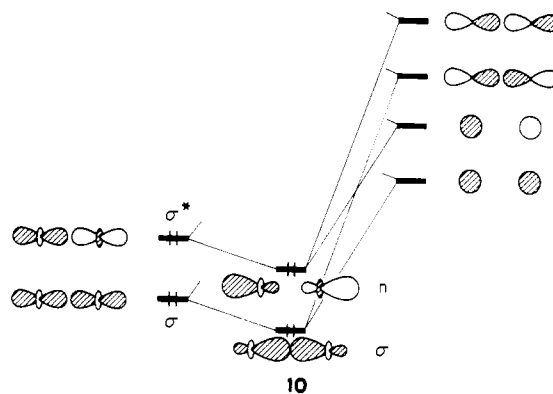
of two-orbital-four-electron repulsive interactions. But on the coppers one also has 4s and 4p valence orbitals. These stabilize both the bonding and antibonding d orbital combinations, as shown schematically in 9.



One can be more specific: The main contributors to Cu–Cu antibonding (if there were only d orbitals on Cu) are the  $\sigma$  and  $\sigma^*$   $z^2$  combinations shown in 10. Admixture of appropriate symmetry-adapted s and z combinations transforms these, increasing the bonding in  $\sigma$  and decreasing the antibonding in  $\sigma^*$ . In the extreme  $\sigma$  becomes a really good bond and  $\sigma^*$  an innocuous lone-pair combination.

The important feature is an admixture of s and p character into predominantly d orbitals, i.e. hybridization. In fact, in valence bond language one could say that the Cu moves from a  $d^{10}$  configuration, which does not allow any bonding, toward a  $d^9s^2p^{1-x}$  configuration. Similar things happen in Ni, Pd, and Pt clusters, aggregating eventually to the metal.

Either way, molecular orbital or valence bond, one reaches the essential conclusion that s and p mixing makes for bonding: the

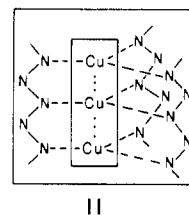


easier such mixing, i.e. the lower down in energy is the s,p set relative to d, the more such bonding one will get. So the Cu(I) story is tied to cluster formation in other closed-shell systems, e.g. in group 2 and 12. There it is  $np$  mixing into  $ns$  that makes for bonding, and one can understand why Be clusters form whereas He ones do not.

### Electronic Structure of $\text{Cu}_3(\text{HNNNNNH})_3$

The model we have chosen for 1 is  $[\text{Cu}(\text{HNNNNNH})]_3$ , with a geometry idealized from the observed structure. The details of the geometry and the extended Hückel calculations used throughout this paper are given in the Appendix. A calculation of this type on the trimer yields a Cu–Cu overlap population of 0.12. So there is a substantial amount of bonding. But where does it come from?

It is natural to think of the Beck and Strähle compound as being formed from an isolated  $\text{Cu}_3^{3+}$  linear array and three tridentate  $\text{HNNNNNH}^-$  ligands, as in 11. The bonding between the

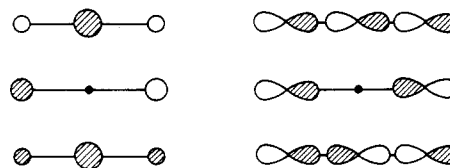


coppers could be there in the  $\text{Cu}_3^{3+}$  unit alone, or it could be induced by the ligands. Table I is illuminating in this respect, for it shows the Cu–Cu overlap population, first in the  $\text{Cu}_3^{3+}$  cluster alone and then in the complex. And in either case we show the effect of including or excluding d or s,p orbitals in the computation.

Looking at the  $\text{Cu}_3^{3+}$  unit alone, one sees essentially the picture outlined in the preceding section: antibonding between coppers if only d orbitals are included, turning into bonding for the complete valence set. Including the ligands has little effect. The interesting point, though, made by the  $\text{Cu}_3(\text{HN}_3\text{H})_3$  "s,p only" entry, is that, even without d orbitals on the copper, the act of bonding with the ligand induces some Cu–Cu bonding.

Let us trace down the origins of this intriguing effect and in the process get some insight into the bonding in 1. Because the emphasis is on the s,p bonding we will introduce that first and then the d orbitals. An interaction diagram for the complex 11 is given in Figure 1, but before we discuss it let us approach the components individually.

$\text{Cu}_3^{3+}$  is at left. Its orbitals are trivially derived, leading to recognizable "allylic" sets such as those shown in 12. There is



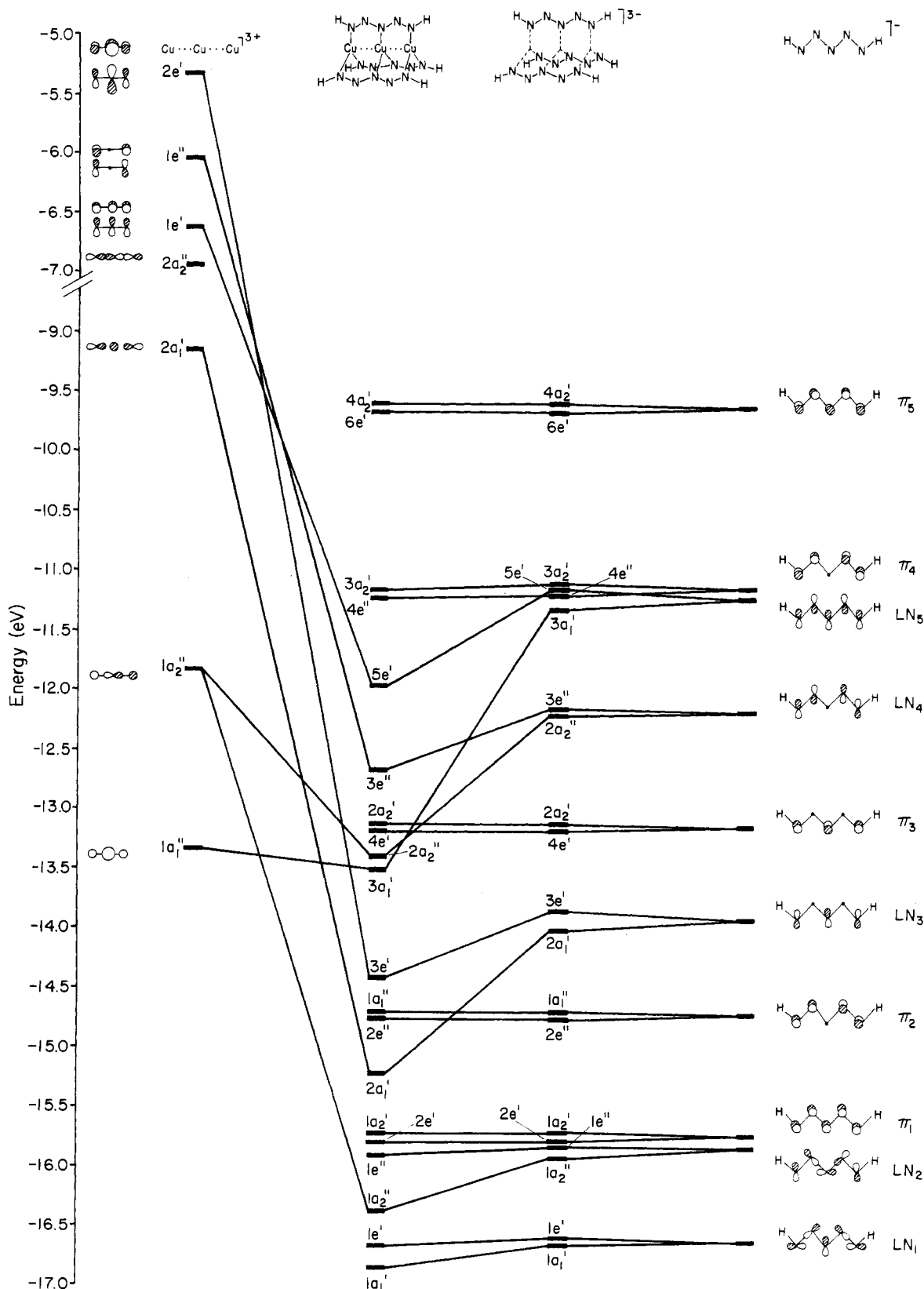


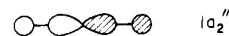
Figure 1. Interaction diagram for 1 (without d orbitals).

Table I. Overlap Populations in  $\text{Cu}_3^{3+}$  and  $\text{Cu}_3(\text{HN}_5\text{H})_3$

cluster	overlap population		
	s,p only	d only	s,p,d
$\text{Cu}_3^{3+}$	(0)	-0.080	+0.132
$\text{Cu}_3(\text{HN}_5\text{H})_3$	+0.055	-0.010	+0.127

also substantial s,p mixing in some of the orbitals. For instance, the low-lying Cu  $1a_2''$  orbital is changed into a combination given

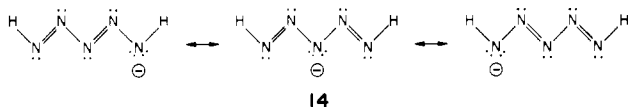
schematically by 13. Formally all of these orbitals are empty in  $\text{Cu}_3^{3+}$ , but we will soon see that they become partially occupied in complexation.



13

For each  $\text{HNNNNNH}^-$  we expect from a valence formula such as 14 that there are five nitrogen lone pairs and five  $\pi$  orbitals

(three occupied) of pentadienyl type. The  $\pi$ 's are easy to find among the valence orbitals of  $\text{HN}_3\text{H}^-$  (at right in Figure 1). The lone pairs are less obvious, because there is of course some mixing with NN and NH  $\sigma$  bonds, but these also can be located; they are labeled  $\text{LN}_{1-5}$  in Figure 1.



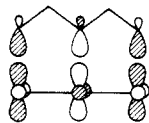
Note that in the free ligand the fifth lone pair combination,  $\text{LN}_5$ , is rather high in energy, perilously close to  $\pi_4$ . One might even predict, if one took the calculation at face value, that the  $\text{HN}_3\text{H}^-$  anion might be a triplet, with an  $(\text{LN}_5)^1(\pi_4)^1$  configuration. There is precious little experimental information on the isolated ligand, which is not very stable. Also it could be the calculations are at fault, for the extended Hückel method tends to put  $\sigma$  levels too high relative to  $\pi$ . MNDO calculations<sup>9</sup> give a larger gap between  $\text{LN}_5$  and  $\pi_4$ . The electronic ambiguity remains interesting, and we will return to some consequences of it when we study some hypothetical polymers. Meanwhile, let us go on to form the complex.

There are three  $\text{HN}_3\text{H}^-$  ligands. They are so far apart in the geometry of **11** that when they are brought together (right side of Figure 1) they interact but little. The threefold symmetry leads to the formation of one nondegenerate and one degenerate orbital from each ligand orbital. Many of the resulting orbitals can form strong interactions with the orbitals from the copper cluster. However, we find, not unexpectedly, that all of the  $\pi$  type ligand orbitals are unable to overlap effectively with any of the copper orbitals. One can see they have approximately or exactly the same energy in the complex as in  $\text{HN}_3\text{H}^-$ .

The ligand lone pairs are stabilized by interaction with empty Cu cluster orbitals. This is, of course, the expected dative bonding. But as a consequence of that mixing, some  $\text{Cu}_3^{3+}$  cluster orbitals get populated, and those that are Cu–Cu bonding get populated more, because they interact more strongly. They are closer to the  $\text{HN}_3\text{H}^-$  ligand orbitals in energy. The most significant  $\text{Cu}_3^{3+}$  fragment molecular orbital populations are 0.92 for  $1a_1'$  and 0.63 for  $1a_2''$ . This is how the ligand induces Cu–Cu bonding.

Note that complex formation has “removed” the near degeneracy of  $\text{LN}_5$  and  $\pi_4$  in the free ligand.  $\text{LN}_5$  has been stabilized; it becomes the  $5e'$  HOMO of the complex. There is about a 0.66-eV gap between HOMO and LUMO in  $\text{Cu}_3(\text{HN}_3\text{H})_3$ , at this stage in the calculation.

We now return the 3d orbitals to Cu. The changes that happen are small. The d block appears in the region around -14 eV in the calculations (Figure 2 shows the changes in the frontier orbital region). There are some significant interactions that are new, e.g. that shown in **15** between  $\text{LN}_3$  and Cu  $x^2-y^2$ . Some  $\pi$  interactions



become effective, for instance interchanging the order of the LUMO's  $4e''$  and  $3a'$ . But the major effect of inclusion of Cu 3d as well as 4s and 4p is a small but significant mixing of s, p, and d on the coppers, just as one found in the  $\text{Cu}_3^{3+}$  case. The  $\text{Cu}_3^{3+}$  fragment MO's  $1a_1'$  and  $1a_2''$  are populated by 0.88 and 0.68 electron, respectively, in the complex.

A weak temperature-independent paramagnetism is observed in the complex.<sup>3</sup> Beck and Strähle conjectured that might be due to a paramagnetic excited state with a radical anion on the ligand and a  $\text{Cu}^{2+}$  ion. Our calculated gap is 0.45 eV. This is not big, but our general experience<sup>10</sup> indicates that a gap of that size is

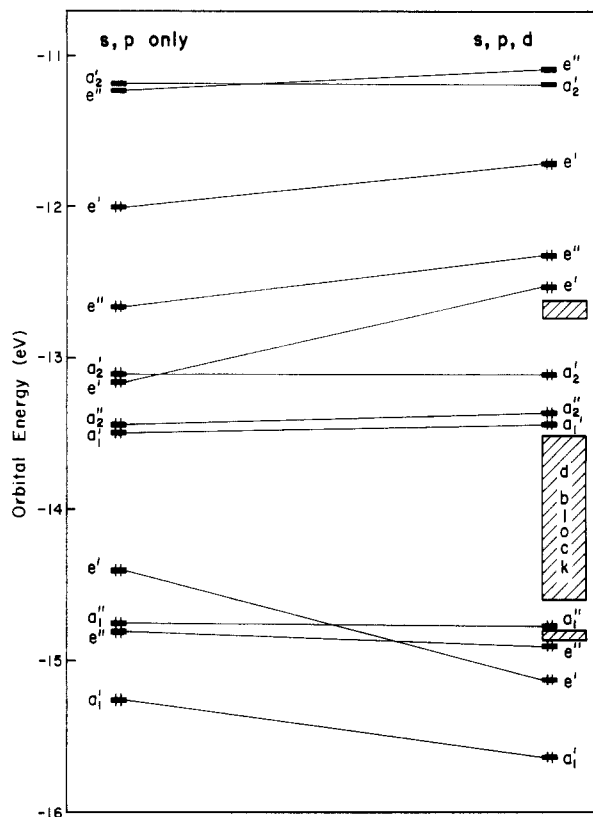
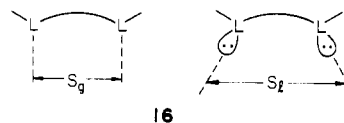


Figure 2. Frontier orbitals for **1** with s,p only (left) and s,p,d (right).

sufficient to guarantee a singlet ground state. Note, incidentally, that promotion of an electron from the  $5e'$  HOMO (some Cu–Cu  $\pi$ -bonding character) to the LUMO (ligand  $\pi$ ) would not provide a mechanism for strengthening the Cu–Cu bond. We have no explanation for the observed paramagnetism.

Since the Cu–Cu interactions are only weakly attractive, while the Cu–ligand interactions are strong, the main factor determining the record short Cu–Cu separation in **1** is the bite size of the ligand. One is tempted to associate that with the distance between the dentate nitrogens in  $\text{RN}_2\text{R}^-$ . That is about 2.2 Å in the experimental geometry, even shorter than the Cu–Cu spacing. But we must not jump too quickly to an identification on the N...N separation with the true bite size: perhaps it is best to distinguish “geometrical” bite size from an “electronic” one. What matters, we think, is the *overlap* between the orbitals emerging from a ligand and the corresponding metal orbitals.<sup>11</sup> The distinction is made clearer, perhaps, in **16**. The geometrical bite size,  $S_g$ ,



is defined by us as simply the distance between the ligands. But what if the lone pairs don't “point” along a perpendicular to the line between the ligands? The maximum overlap with some metal orbitals might then come at a larger or smaller distance  $S_e$ , the electronic bite size. And just to make things complicated,  $S_e$  could depend on the metal–ligand separation.

It is not easy to define  $S_e$ , since the definition is theoretical and not experimental and one has to specify the metal orbitals interacting with the ligand. The matter merits a separate study, for a variety of ligands. But in the case at hand what we did was to take a single ligand and one Cu atom (s,p,d) placed 2.03 Å

(9) Dewar, M. J. S.; Thiel, W. *J. Am. Chem. Soc.* **1977**, *99*, 4907.

(10) See, e.g., the discussion in: Hay, P. J.; Thibault, J. C.; Hoffmann, R. *J. Am. Chem. Soc.* **1975**, *97*, 4484.

(11) For a review, see: Moore, D. S.; Robinson, S. D. *Adv. Inorg. Chem. Radiochem.* **1986**, *30*, 1.

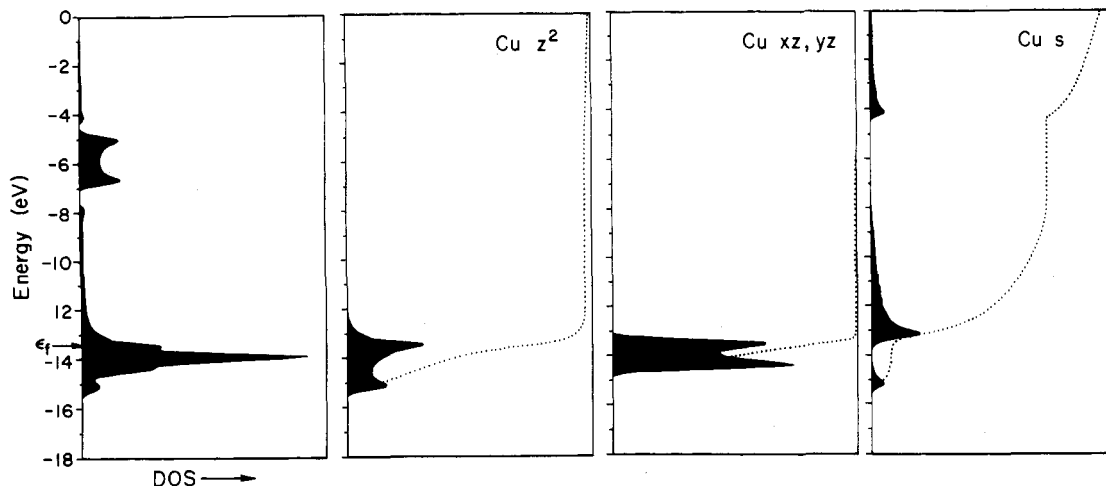
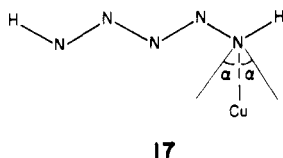


**Figure 3.** For a  $\text{Cu}_\infty$  rod, from left to right: (a) total density of states; (b)  $z^2$  contribution to DOS; (c)  $xz, yz$  contribution; (d)  $s$  contribution. Parts b-d are magnified by a factor of 3.0.

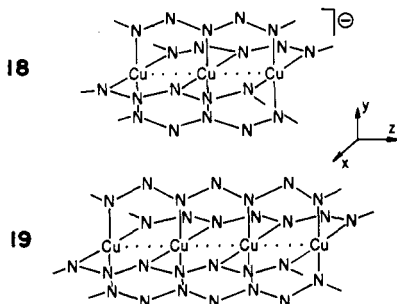
away from the nitrogen. We then moved it on an arc measured by an angle  $\alpha$  (17), keeping Cu-N constant. The optimum  $\alpha$  is



1°, pretty close to zero. So in this case the electronic bite size is nearly the same as the geometric one.

#### Other Oligomers and Polymers

It is obviously possible to imagine four pentaazenido groups around a  $\text{Cu}_3$  bar (18). There exist analogous triazenido binuclear complexes  $\text{M}_2(\text{RN}_3\text{R})_4$ .<sup>11</sup> And it is possible to hypothesize extended analogues of 1 and 18 with new ligands,  $\text{RN}_x\text{R}$ , e.g. 19. The problem is not in thinking these molecules up or in doing calculations on them, but in synthesizing them.



Calculations on 18 and 19 yield few surprises. The square-planar crystal field around each Cu is characteristically strong. It pushes one d orbital,  $x^2 - y^2$  ( $z$  is the Cu...Cu axis) on each center way up in energy. If the electron count were as shown, the destabilized electrons would enter N-N antibonding ligand  $\pi^*$  orbitals. Oxidation of the molecule as a whole (and so of the Cu centers to  $\text{Cu}^{2+}$  or  $\text{Cu}^{3+}$ ) is more likely.

Polymeric extrapolations of 1 or 18 and 19 spring to mind. The unit cells of these are shown in 20 and 21. The ligand in these

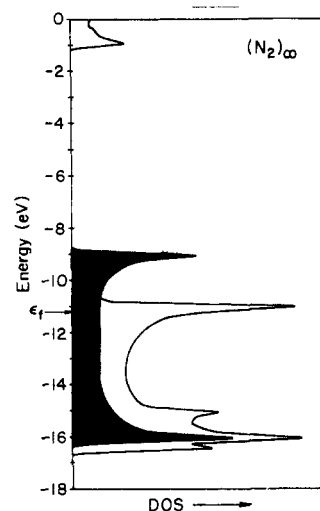
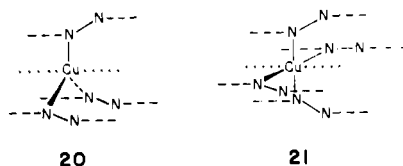
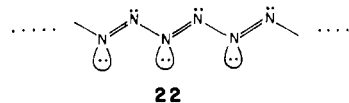


**Figure 4.** Calculated total DOS and the  $p_z$  projection for  $(\text{N}_2)_\infty$ .

polymers should be formally neutral, if it is to provide the same lone pair and  $\pi$  environment as  $\text{RN}_3\text{R}^-$  and  $\text{RN}_5\text{R}^-$  (22). So the



electron counts one might focus on would be those corresponding to  $\text{Cu}(\text{N}_2)_3^+$  in 20, and (given the strong square-planar crystal field)  $\text{Cu}(\text{N}_2)_4^{2,3+}$  in 21.

Let us focus first on the  $\text{Cu}_\infty$  rod that is found in both 20 and 21. The band structure of a linear chain is pretty simple.<sup>12</sup> Decomposition of the density of states (DOS), shown in Figure 3, show the following:

(1) A metal d block, consisting of a wide  $z^2$  or  $\sigma$  band, a narrower  $xz, yz$  or  $\pi$  band, and a very undispersed  $x^2 - y^2, xy$ , or  $\delta$  band is observed.

(2) There is strong  $s, p_z$  mixing, resulting in a Cu-Cu  $\sigma$  bonding band (-8 to -13 eV) and a higher lying  $\sigma^*$ , Cu-Cu antibonding band.<sup>12</sup> The  $x, y$  band is much less dispersed, around -6 eV.

(3) There is clear evidence of the same  $s, p, d$  mixing that we found so important in  $\text{Cu}_2^{2+}$  and  $\text{Cu}_3^{3+}$ : note the "resonances" between  $z^2$  and  $s$  contributions at -15 and -13 eV.

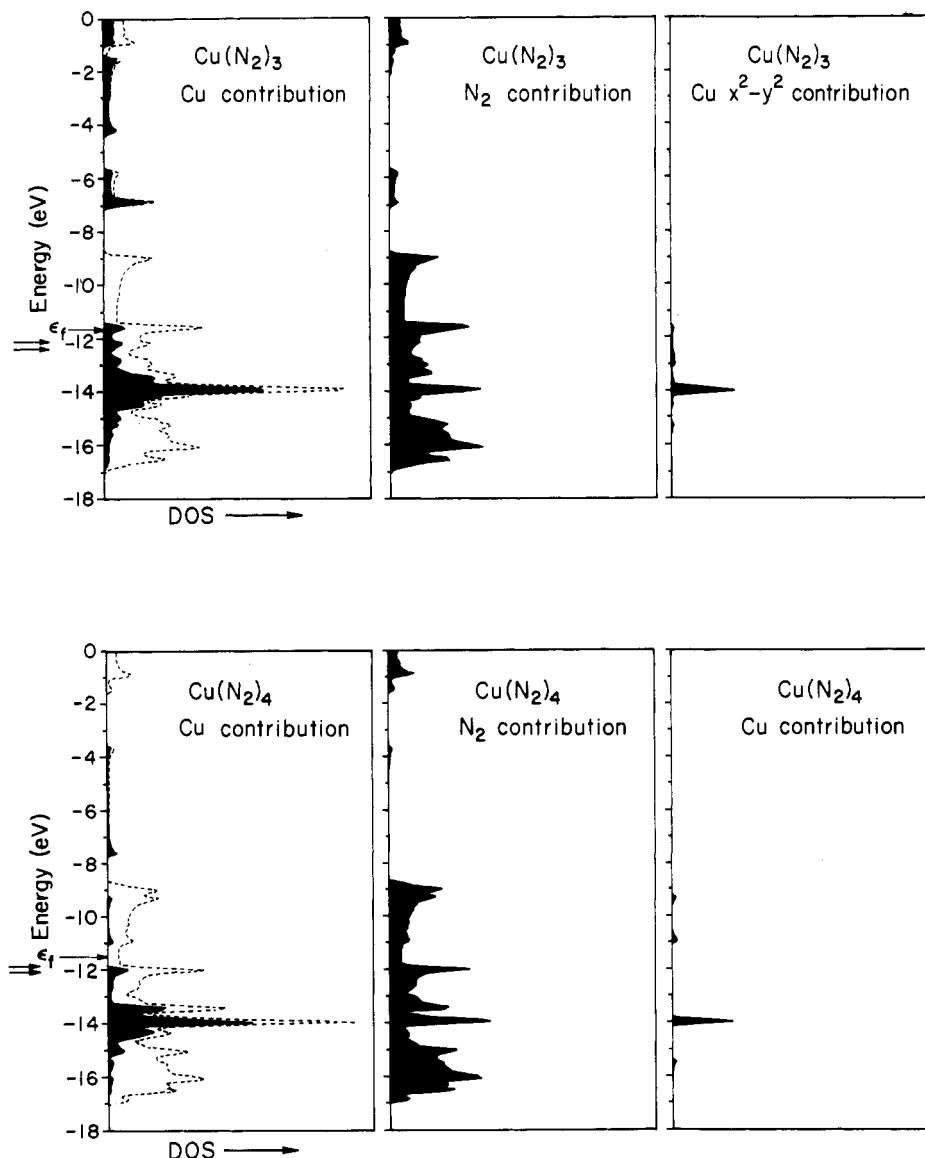


**Figure 5.** Calculated DOS plots for the Cu orbitals, all N orbitals, and  $d_{x^2-y^2}$  type orbitals for (a) **20** and (b) **21**. The Fermi level is indicated for unit cell electron counts of 40, 39, and 38 for **20**, while for **21** they are 50, 49, and 48.

Figure 4 shows the computed density of states of the  $(N_2)_\infty$  ligand polymer itself, along with the  $\pi$  contributions to it. The wide  $\pi$  band is what one would expect of the polyene analogue.

Tripling or quadrupling this polymer, as one must to form **20** or **21**, will not do much to the DOS. But interaction with the Cu chain has more serious effects. Selected contributions to the DOS for the composite polymers **20** and **21** are shown in Figure 5.

The following points may be noted:

(1) These molecules should be conducting, for most reasonable electron counts. The possibility exists, however, that for electron counts close to  $Cu^{2+}$ , these polymers might be antiferromagnetically coupled, as in the familiar copper acetates.<sup>13</sup>

(2) The Fermi level comes in a region of mainly  $(N_2)_\infty$  ligand states, both  $\sigma$  (lone pair) and  $\pi$ . Recall that even in the  $Cu_3-(RN_3R)_3$  complex there was already a small gap between  $\pi_4$  and  $LN_5 + \lambda Cu$  combinations. As the ligand chain is extended that gap must vanish—the  $\pi$  levels and the lone pair levels develop into a band.

(3) Crystal field effects are apparent: note the low energy of the  $x^2 - y^2$  contribution in the trigonally coordinated  $Cu(N_2)_3$  polymer, contrasted with the high energy of these orbitals in the

square-planar  $Cu(N_2)_4$  environment.

**Acknowledgment.** We thank J. Strähle for the impetus for this work, and for providing some experimental information prior to publication. K.M.M. would like to thank Ralph Wheeler, Marja Zonneville, and Jing Li for enlightening conversations regarding this research. Jing Li is to be especially thanked for reproducing some of the calculations at Cornell and sending the results over BITNET to Lund University, Lund, Sweden. We are grateful to the Swedish National Research Council for a Tage Erlander Professorship, which made our stay at the Kemcentrum in Lund possible. We thank Prof. Sten Andersson and his group for their hospitality. Our research at Cornell was generously supported by the National Science Foundation through Research Grant DMR821722702 to the Materials Science Center. We are grateful to Jane Jorgensen and Elisabeth Fields for their expert drawings.

#### Appendix

The extended Hückel method<sup>14</sup> in the tight binding approximation<sup>15</sup> was used in all calculations. The parameters used for carbon, hydrogen, and copper were as follows:  $H_{ss} = -26.0$  eV,  $H_{pp} = -13.4$  eV,  $\zeta_{s,p} = 1.95$ ;  $H_{ss} = -13.6$  eV,  $\zeta_{s,p} = 1.3$ ;  $H_{ss} = -11.4$

(13) For a leading reference, see: Harcourt, R. D.; Skrezenek, F. L.; Macclagan, R. G. A. *R. J. Am. Chem. Soc.* **1986**, *108*, 5403.

(14) Hoffmann, R. *J. Chem. Phys.* **1963**, *39*, 1397. Hoffmann, R.; Lipscomb, W. N. *J. Chem. Phys.* **1963**, *36*, 3179; **1962**, *37*, 2872.

(15) Whangbo, M.-H.; Hoffmann, R. *J. Am. Chem. Soc.* **1978**, *100*, 6093.

eV,  $H_{pp} = -6.06$  eV,  $H_{dd} = -14.0$  eV,  $\zeta_{s,p} = 2.2$ ,  $\zeta_{d1} = 5.95$ ,  $\zeta_{d2} = 2.3$ ,  $c_1 = 0.5933$ ,  $c_2 = 0.5744$  respectively. To calculate average properties for the 1-D cases a 100-point k-point set was used.<sup>16</sup> The geometries used for calculations were as follows: Cu-Cu-

(monomer), 2.35 Å; Cu-Cu(polymer), 2.26 Å; N-N, 1.34 Å; Cu-N, 2.03 Å; N-H, 1.0 Å; Cu-N-N, 122.5°; N-N-N, 115.0°; H-N-N, 118.0°.

**Registry No.** [Cu(tolylN(N)N(N)Ntolyl)]<sub>3</sub>, 96129-16-7; [Cu<sub>3</sub>(tolylN(N)N(N)Ntolyl)<sub>4</sub>]<sup>-</sup>, 114326-40-8; [Cu(tolylN(N)N(N)N(N)Ntolyl)]<sub>4</sub>, 114350-60-6.

(16) Pack, J. D.; Monkhorst, J. H. *Phys. Rev. B: Solid State* 1977, 16, 1748.

Contribution from the Department of Chemistry and Laboratory for Molecular Structure and Bonding, Texas A&M University, College Station, Texas 77843

## Preparation and Properties of the Mo<sub>2</sub>X<sub>4</sub>(PMe<sub>3</sub>)<sub>4</sub> Compounds with X = NCS and NCO

F. Albert Cotton\* and Marek Matusz

Received January 20, 1988

The Mo<sub>2</sub>X<sub>4</sub>(PMe<sub>3</sub>)<sub>4</sub> compounds where X = NCO and NCS are formed in a high-yield, one-pot reaction from Mo<sub>2</sub>(O<sub>2</sub>CCH<sub>3</sub>)<sub>4</sub> and (CH<sub>3</sub>)<sub>3</sub>SiX in the presence of the phosphine. Both compounds crystallize in the tetragonal space group *P*4<sub>2</sub>,<sub>2</sub> with the following unit cell dimensions. X = NCO:  $a = b = 11.990$  (2) Å,  $c = 20.271$  (2) Å,  $V = 2914$  (1) Å<sup>3</sup>,  $Z = 4$ . X = NCS:  $a = b = 12.556$  (1) Å,  $c = 21.033$  (4) Å,  $V = 3316$  (1) Å<sup>3</sup>,  $Z = 4$ . Both molecules consist of quadruply bonded molybdenum atoms with trans phosphines and X groups as ligands. Electrochemical and spectroscopic properties of these compounds have been investigated and correlated with other compounds where X = Cl, Br, and I.

### Introduction

Mo<sub>2</sub>X<sub>4</sub>L<sub>4</sub> complexes are among the most often studied multiple-bonded dimetal complexes. They have contributed much to the understanding of the nature of the multiple bonds between metal atoms.<sup>1</sup> In the past, conclusions have been drawn on some incomplete classes of these compounds. Recently the discovery of some new compounds, namely Mo<sub>2</sub>I<sub>4</sub>(PMe<sub>3</sub>)<sub>4</sub><sup>2</sup> and Mo<sub>2</sub>I<sub>4</sub>(dppe)<sub>2</sub>,<sup>3</sup> has shed some new light on the subject. The Mo<sub>2</sub>X<sub>4</sub>(PMe<sub>3</sub>)<sub>4</sub> (X = Cl, Br, I) set has received the most attention, because of the simplicity of the system, but two other classes, Mo<sub>2</sub>X<sub>4</sub>(dppe)<sub>2</sub> (X = Cl, Br, I) and Mo<sub>2</sub>X<sub>4</sub>(dppm)<sub>2</sub> (X = Cl, Br, I, NCS), have also been investigated and structurally characterized. In view of their theoretical importance, we decided to extend the Mo<sub>2</sub>X<sub>4</sub>(PMe<sub>3</sub>)<sub>4</sub> series with some new compounds. As a part of our recent interest<sup>4</sup> in the thiocyanate chemistry of M<sub>2</sub> species, we have prepared Mo<sub>2</sub>(NCS)<sub>4</sub>(PMe<sub>3</sub>)<sub>4</sub>. By the same synthetic route Mo<sub>2</sub>(NCO)<sub>4</sub>(PMe<sub>3</sub>)<sub>4</sub> was also prepared. These two compounds, together with the Cl, Br, and I derivatives, form the largest known class of quadruply bonded, homologous compounds. In this study we report the preparation and molecular structures of these two new compounds, as well as their spectroscopic and electrochemical properties. The relationship between the energy of the  $\delta$ - $\delta^*$  transition and the first reduction potential for the entire class has been examined.

### Experimental Section

All reactions were done under anaerobic conditions. Me<sub>3</sub>SiNCO and Me<sub>3</sub>SiNCS were purchased from Aldrich Chemical Co. Trimethylphosphine was purchased from Strem Chemicals Inc.

**Preparation of Mo<sub>2</sub>(NCO)<sub>4</sub>(PMe<sub>3</sub>)<sub>4</sub> (1).** A round-bottom flask was charged with 1.0 g (2.3 mmol) of Mo<sub>2</sub>(O<sub>2</sub>CCH<sub>3</sub>)<sub>4</sub>, 0.858 g (11 mmol) of PMe<sub>3</sub>, 1.26 g (11 mmol) of Me<sub>3</sub>SiNCO, and 50 mL of toluene. The reaction mixture was stirred at room temperature for 2 days and then evaporated to dryness. The solid residue was dissolved in hot toluene (about 150 mL), and the mixture was filtered hot through a short Celite column. The solution was refrigerated overnight to give well-formed crystals of the product, which were filtered out, washed with hexane, and vacuum-dried. The yield was 1.2 g (72% based on Mo) of blue-black

crystals. They are soluble in THF, benzene, and CH<sub>2</sub>Cl<sub>2</sub> to give sky blue solutions. The compound can be handled in the air in the solid state but decomposes slowly in solution. UV-vis (CH<sub>2</sub>Cl<sub>2</sub> solution):  $\lambda = 617$  nm ( $\epsilon = 8050$  M<sup>-1</sup> cm<sup>-1</sup>),  $\lambda = 460$  nm ( $\epsilon = 430$  M<sup>-1</sup> cm<sup>-1</sup>),  $\lambda = 330$  nm ( $\epsilon = 12370$  M<sup>-1</sup> cm<sup>-1</sup>). The same  $\lambda_{max}$  values were recorded for the THF solution of the compound. IR (cm<sup>-1</sup>): 2210 vs, 1380 m, 1345 m, 1305 m, 1290 m, 960 s, 865 w, 855 w, 750 m, 680 m, 620 m, 380 m. <sup>31</sup>P NMR: -8.30 ppm (s).

**Mo<sub>2</sub>(NCS)<sub>4</sub>(PMe<sub>3</sub>)<sub>4</sub> (2).** The experimental procedure is essentially the same as that described above. Isolated yields were typically 80% of a dark green crystalline solid. Solubility and stability are similar to those of the NCO derivative. UV-vis (CH<sub>2</sub>Cl<sub>2</sub> solution):  $\lambda = 670$  nm ( $\epsilon = 6680$  M<sup>-1</sup> cm<sup>-1</sup>),  $\lambda = 497$  nm ( $\epsilon = 380$  M<sup>-1</sup> cm<sup>-1</sup>),  $\lambda = 395$  nm ( $\epsilon = 23100$  M<sup>-1</sup> cm<sup>-1</sup>). IR (cm<sup>-1</sup>): 2040 vs, 1380 m, 1310 m, 1290 m, 960 s, 870 m, 810 m, 805 m, 750 m, 745 m, 625 m, 490 m, 360 m. <sup>31</sup>P NMR: -6.8 ppm (s). Anal. Calcd for Mo<sub>2</sub>S<sub>2</sub>P<sub>4</sub>N<sub>4</sub>C<sub>16</sub>H<sub>36</sub>: C, 26.40; H, 4.98; N, 7.69. Found: C, 26.65; H, 5.08; N, 7.54.

Mo<sub>2</sub>(NCS)<sub>4</sub>(PMe<sub>3</sub>)<sub>4</sub> could also be prepared by an alternative procedure: Mo<sub>2</sub>Cl<sub>4</sub>(PMe<sub>3</sub>)<sub>4</sub>, 0.20 g (0.313 mmol), KSCN, 0.122 g (1.25 mmol), and 15 mL of MeOH were refluxed for 24 h. The reaction mixture turned from fluorescent red-blue to green during this time. It was cooled and filtered. The solid residue was washed with a small amount of MeOH and extracted with boiling toluene. The toluene solution was filtered hot through a Celite bed and refrigerated. Next day the crystalline product was filtered out and vacuum-dried. The yield was 0.144 g (53%). The spectroscopic (UV-vis, <sup>31</sup>P NMR) and electrochemical properties were identical with those of the sample obtained by the Me<sub>3</sub>SiNCS method.

We were unable to obtain Mo<sub>2</sub>(NCO)<sub>4</sub>(PMe<sub>3</sub>)<sub>4</sub> by the similar ligand-exchange reaction.

**Measurements.** Elemental analyses were performed by Galbraith Laboratories Inc. IR spectra were recorded as Nujol mulls on KBr plates (4000-600 cm<sup>-1</sup>) or CsI plates (600-300 cm<sup>-1</sup>) with a Perkin-Elmer 785 spectrophotometer. The electronic spectra were recorded on dichloromethane solutions (Aldrich, HPLC grade) with a Cary 17D spectrophotometer. Electrochemical measurements were done with a BAS-100 electrochemical analyzer, employing 0.2 M tetra-*n*-butylammonium hexafluorophosphate solutions in THF or CH<sub>2</sub>Cl<sub>2</sub>. A three-electrode configuration was used with platinum working and auxiliary electrodes and a silver-silver chloride reference electrode. The potentials are corrected for the solution resistance. Under the experimental conditions, ferrocene is oxidized at  $E_{1/2} = 0.510$  V in CH<sub>2</sub>Cl<sub>2</sub> and  $E_{1/2} = 0.595$  V in THF. <sup>31</sup>P NMR samples were recorded on CDCl<sub>3</sub> solutions with a Varian XL 200 spectrometer and are referenced to 85% H<sub>3</sub>PO<sub>4</sub>.

### X-ray Crystallography

Single crystals of compounds 1 and 2, obtained as described in the experimental section, were glued on top of glass fibers. Indexing revealed tetragonal cells, Laue class (*4/mmm*), and axial dimensions were con-

- Cotton, F. A.; Walton, R. A. *Multiple Bonds Between Metal Atoms*; Wiley: New York, 1982.
- Hopkins, M. D.; Schaefer, W. D.; Bronikowski, M. J.; Woodruff, W. H.; Miskowski, V. M.; Dallinger, R. F.; Gray, H. B. *J. Am. Chem. Soc.* 1987, 109, 408. Cotton, F. A.; Poli, R. *Inorg. Chem.* 1987, 26, 3228.
- Cotton, F. A.; Dunbar, K. R.; Matusz, M. *Inorg. Chem.* 1986, 25, 3641.
- Cotton, F. A.; Matusz, M. *Inorg. Chem.* 1987, 26, 3468.